Time-correlated Window Carrier-phase Aided GNSS Positioning in Urban Canyons

Xiwei Bai(**Presenter**), Weisong Wen *, Li-Ta Hsu

Department of Aeronautical and Aviation Engineering
The Hong Kong Polytechnic University

For group meeting, 2022

Challenges of Positioning in Urban Areas

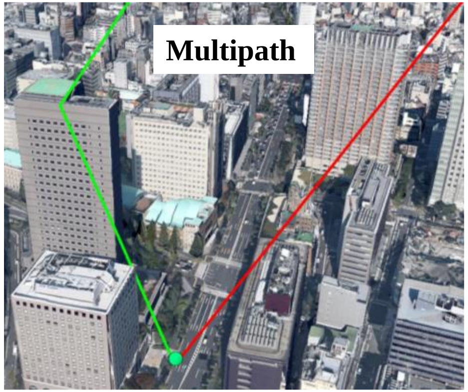

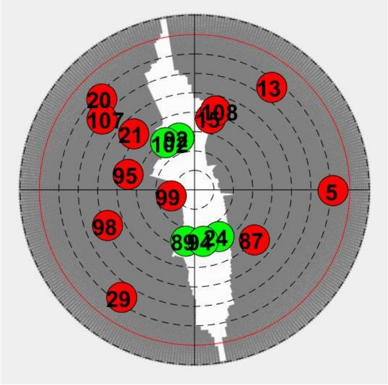

GNSS positioning is challenged due to signal blockage and reflection!

How to improve the GNSS positioning in urban areas?

Code vs Carrier-Based Positioning

	Standard Positioning (code-based)	Precise Positioning (carrier-based)
Observables	Pseudorange (Code)	**Carrier-Phase + Pseudorange**
Receiver Noise	30 cm	3 mm
Multipath	30 cm - 30 m	1 - 3 cm
Sensitivity	High (<20dBHz)	Low (>35dBHz)
Discontinuity	No Slip	Cycle-Slip
Ambiguity	-	Estimated/Resolved
Receiver	Low-Cost (~$100)	**Expensive (~$20,000)**
Accuracy (RMS)	3 m (H), 5 m (V) (Single) 1 m (H), 2 m (V) (DGPS)	**5 mm (H), 1 cm (V) (Static) 1 cm (H), 2 cm (V) (RTK)**
Application	Navigation, Timing, SAR,...	Survey, Mapping, ...

Source: RTK-AlgorithmAn-Lin-Tao-2015

If good carrier-phase is available, what FGO can do!

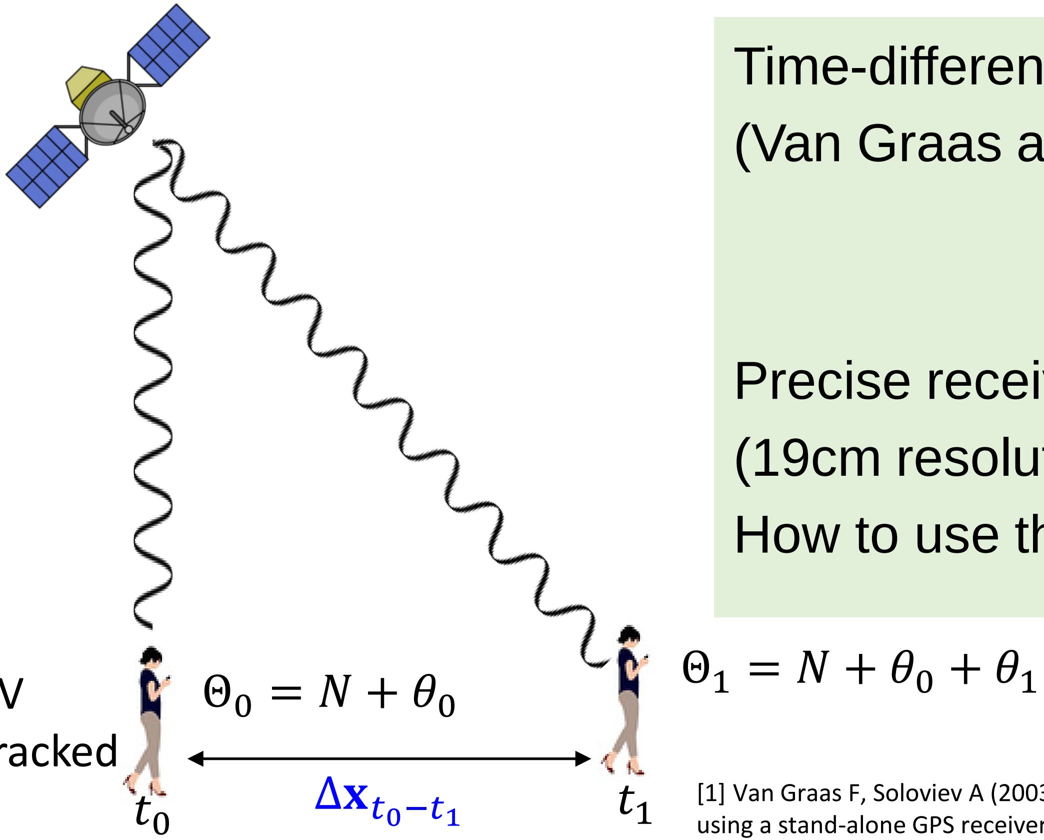

Time-differenced carrier phase (TDCP) [1]
(Van Graas and Soloviev 2003)

$$(\Theta_1 - \Theta_0) = \theta_1$$

$$\theta_1 = g \cdot \Delta\mathbf{x}_{t_0 - t_1}$$

Precise receiver velocity estimation!
(19cm resolution!)
How to use this TDCP in FGO?

[1] Van Graas F, Soloviev A (2003) Precise velocity estimation using a stand-alone GPS receiver. In: Proc. ION NTM 2003,

Framework of Conventional Method (TDCP)

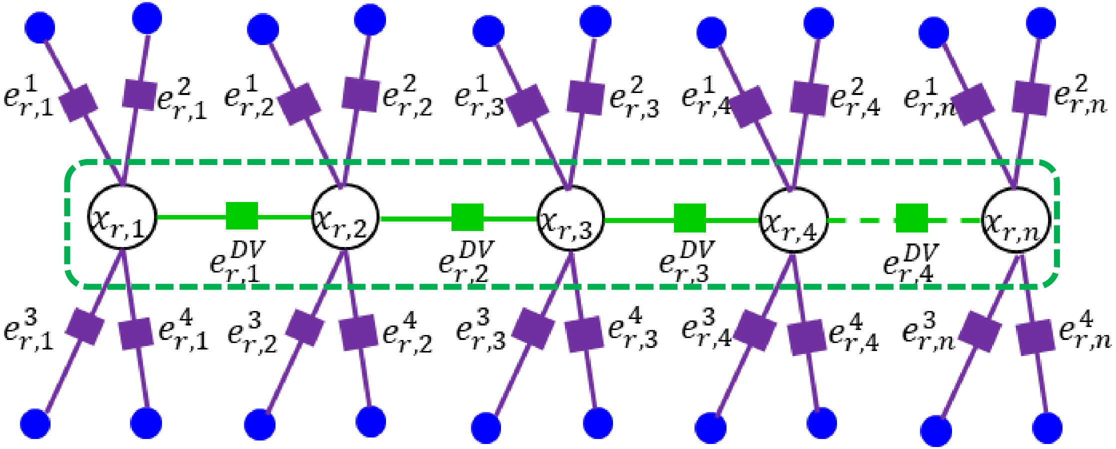

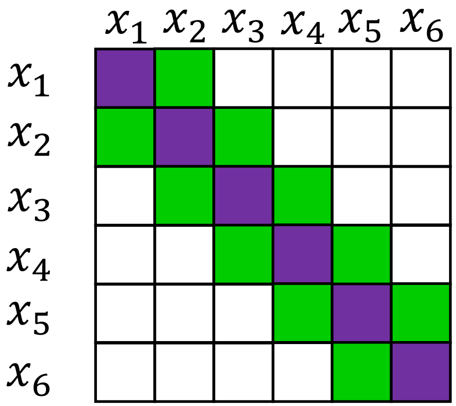

Cross-correlation Matrix

$x_{r,1}$ State node: GNSS receiver ● Satellite ■ Pseudorange Factor: $e_{r,t}^{s}$

■ Doppler Velocity Factor: $e_{r,t}^{DV}$

$$\left|\mathbf{e}_{r,t}^{DV}\right|_{\boldsymbol{\Sigma}_{r,t}^{DV}}^{2} = \left|\frac{\mathbf{v}_{r,t}^{DV} + \mathbf{v}_{r,t+1}^{DV}}{2} - h_{r,t}^{DV}\left(\mathbf{x}_{r,t+1}, \mathbf{x}_{r,t}\right)\right|_{\boldsymbol{\Sigma}_{r,t}^{DV}}^{2}$$

$e_{r,t}^{DV}$ can considers two neighboring epochs

Framework of Conventional Method (TDCP)

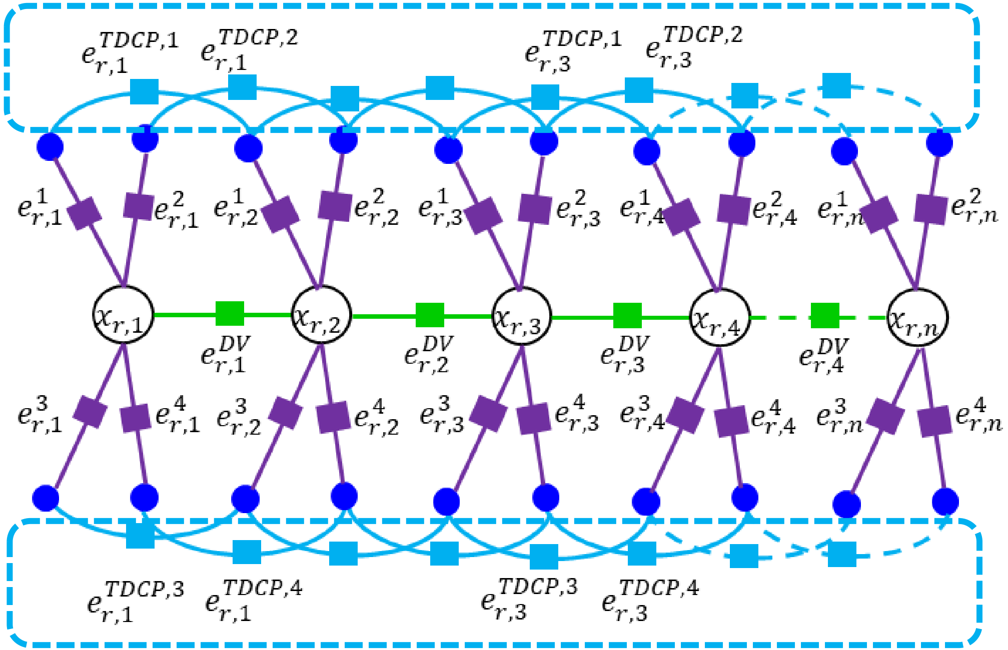

$x_{r,1}$ State node: GNSS receiver · Satellite · Pseudorange Factor: $e_{r,t}^{s}$

Doppler Velocity Factor: $e_{r,t}^{DV}$ · TDCP Factor: $\mathbf{e}_{r,t}^{TDCP,s}$

Time-differenced carrier phase (TDCP)

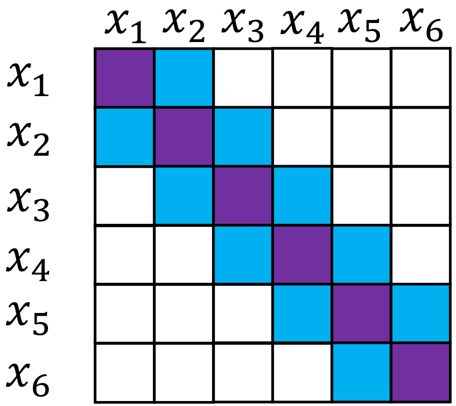

Cross-correlation Matrix

TDCP only considers two neighboring epochs

TDCP measurement modeling

$$\Delta\lambda\psi_{r,t,t+1}^{s} = (r_{r,t+1}^{s} - r_{r,t}^{s}) + c_L(\delta_{r,t+1} - \delta_{r,t}) + (\epsilon_{r,t+1}^{s} - \epsilon_{r,t}^{s})$$

Framework of Conventional Method (TDCP)

$$\lambda\psi_{r,t}^{s} = r_{r,t}^{s} + c_L(\delta_{r,t} - \delta_{r,t}^{s}) - I_{r,t}^{s} + T_{r,t}^{s} + \lambda B_{r,t}^{s} + d\psi_{r,t}^{s} + \epsilon_{r,t}^{s}$$

carrier-phase bias: $B_{r,t}^{s} = \psi_{r,0,t} - \psi_{0,t}^{s} + N_{r,t}^{s}$

carrier-phase integer ambiguity: $N_{r,t}^{s}$

TDCP measurement modeling

$$\Delta\lambda\psi_{r,t,t+1}^{s} = (r_{r,t+1}^{s} - r_{r,t}^{s}) + c_L(\delta_{r,t+1} - \delta_{r,t}) + (\epsilon_{r,t+1}^{s} - \epsilon_{r,t}^{s})$$

$$\Delta\lambda\psi_{r,t,t+1}^{s} = h_{r,t}^{TDCP,s}(\mathbf{p}_{r,t}, \mathbf{p}_{t}^{s}, \delta_{r,t}, \mathbf{p}_{r,t+1}, \mathbf{p}_{t+1}^{s}, \delta_{r,t+1}) + \omega_{r,t}^{TDCP,s}$$

$$\left|\mathbf{e}_{r,t}^{TDCP,s}\right|_{\boldsymbol{\Sigma}_{r,t}^{TDCP,s}}^{2} = \left|\Delta\lambda\psi_{r,t,t+1}^{s} - h_{r,t}^{TDCP,s}(\mathbf{p}_{r,t}, \mathbf{p}_{t}^{s}, \delta_{r,t}, \mathbf{p}_{r,t+1}, \mathbf{p}_{t+1}^{s}, \delta_{r,t+1})\right|_{\boldsymbol{\Sigma}_{r,t}^{TDCP,s}}^{2}$$

Time-differenced carrier phase (TDCP)

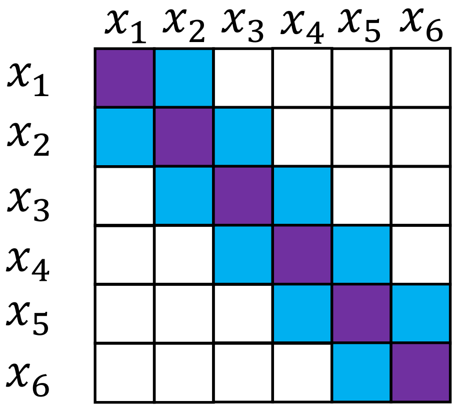

Cross-correlation Matrix

Limitation： TDCP only considers two neighboring epochs

According to the nature of GNSS tracking loops, **the integer ambiguity tends to be constant** when the satellite is **effectively tracked !**

Framework of Proposed Method

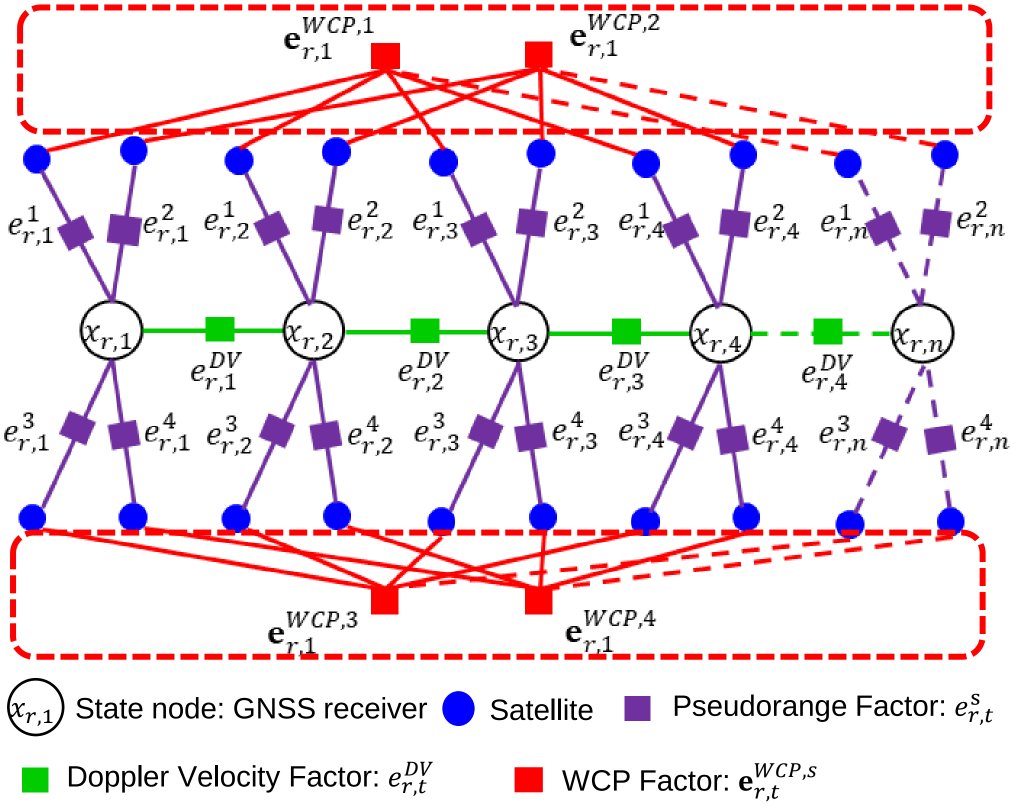

WCP can explore the kinematic time-correlation between multiple epochs

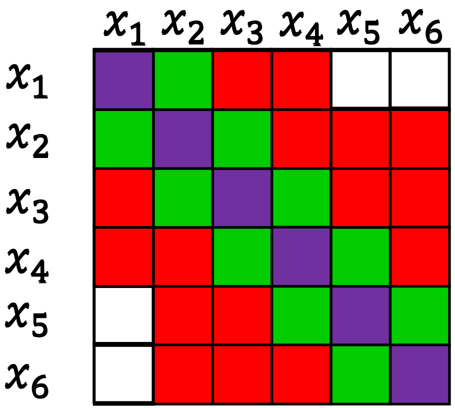

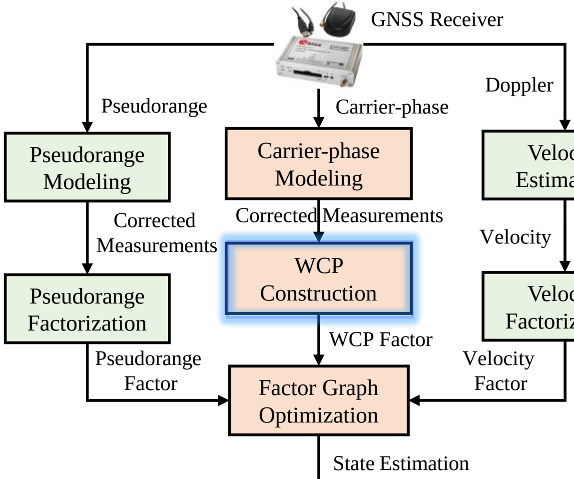

Factor Graph Structure (Pseudorange/Doppler/WCP)

The proposed method: Window Carrier Phase

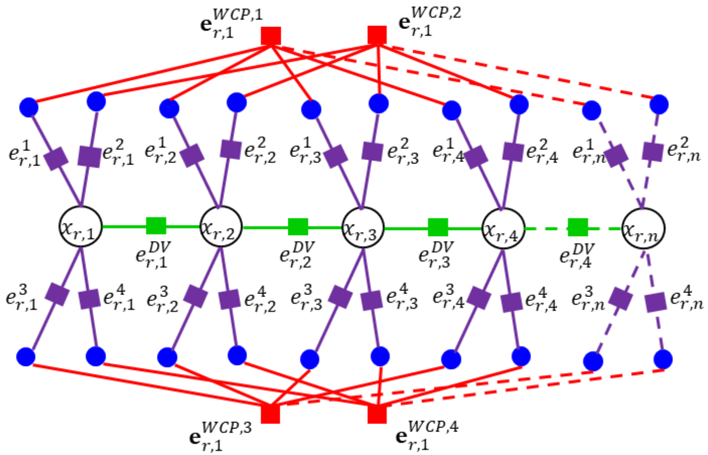

The continuous observed carrier-phase measurements between multiple epochs:

$$\begin{bmatrix} \lambda\psi_{r,1}^{1} \\ \lambda\psi_{r,2}^{1} \\ \dots \\ \lambda\psi_{r,N_k^s}^{1} \end{bmatrix} = \begin{bmatrix} r_{r,t}^{s} + m_{r,1}^{s} \\ r_{r,2}^{s} + m_{r,2}^{s} \\ \dots \\ r_{r,N_k^s}^{s} + m_{r,N_k^s}^{s} \end{bmatrix} + \begin{bmatrix} \lambda B_{r,1}^{s} \\ \lambda B_{r,2}^{s} \\ \dots \\ \lambda B_{r,N_k^s}^{s} \end{bmatrix} + \begin{bmatrix} \epsilon_{r,1}^{s} \\ \epsilon_{r,2}^{s} \\ \dots \\ \epsilon_{r,N_k^s}^{s} \end{bmatrix}$$

With $m_{r,t}^{s} = c_L(\delta_{r,t} - \delta_{r,t}^{s}) - I_{r,t}^{s} + T_{r,t}^{s} + d\psi_{r,t}^{s}$

$$\begin{bmatrix} \lambda\psi_{r,1}^{1} \\ \lambda\psi_{r,2}^{1} \\ \dots \\ \lambda\psi_{r,N_k^s}^{1} \end{bmatrix} = \begin{bmatrix} r_{r,t}^{s} + m_{r,1}^{s} \\ r_{r,2}^{s} + m_{r,2}^{s} \\ \dots \\ r_{r,N_k^s}^{s} + m_{r,N_k^s}^{s} \end{bmatrix} + \lambda B_{r,N_k^s}^{s} \begin{bmatrix} 1 \\ 1 \\ \dots \\ 1 \end{bmatrix} + \begin{bmatrix} \epsilon_{r,1}^{s} \\ \epsilon_{r,2}^{s} \\ \dots \\ \epsilon_{r,N_k^s}^{s} \end{bmatrix}$$

[1] left null space matrix $\mathbf{G}_{r,k}^{s}$

$$\mathbf{G}_{r,k}^{s} \begin{bmatrix} \lambda\psi_{r,1}^{1} \\ \lambda\psi_{r,2}^{1} \\ \dots \\ \lambda\psi_{r,N_k^s}^{1} \end{bmatrix} = \mathbf{G}_{r,k}^{s} \begin{bmatrix} r_{r,t}^{s} + m_{r,1}^{s} \\ r_{r,2}^{s} + m_{r,2}^{s} \\ \dots \\ r_{r,N_k^s}^{s} + m_{r,N_k^s}^{s} \end{bmatrix} + \mathbf{G}_{r,k}^{s} \begin{bmatrix} \epsilon_{r,1}^{s} \\ \epsilon_{r,2}^{s} \\ \dots \\ \epsilon_{r,N_k^s}^{s} \end{bmatrix}$$

[1] Watkins D S. Fundamentals of matrix computations[M]. John Wiley & Sons, 2004.

$\mathbf{p}_{r,N_k^s}$: receiver *r* position
$\mathbf{p}_{N_k^s}^{s}$: satellite s position
$\delta_{N_k^s}$: the clock bias
$B_{r,N_k^s}^{s}$: the shared integer ambiguity
$d\psi_{r,t}^{s}$: the carrier phase correction
$\epsilon_{r,t}^{s}$: the errors caused by multipath

The N_k^s indicates that satellite 1 is tracked continuously for N_k^s epochs

$\mathbf{\Sigma}_{r,k}^{WCP,s}$ and $\mathbf{\Sigma}_{r,k}^{TDCP,s}$ denote **covariance matrix** calculated by the satellite elevation angle, signal, and noise ratio

Factor Graph Structure (Pseudorange/Doppler/WCP)

The proposed method: Window Carrier Phase

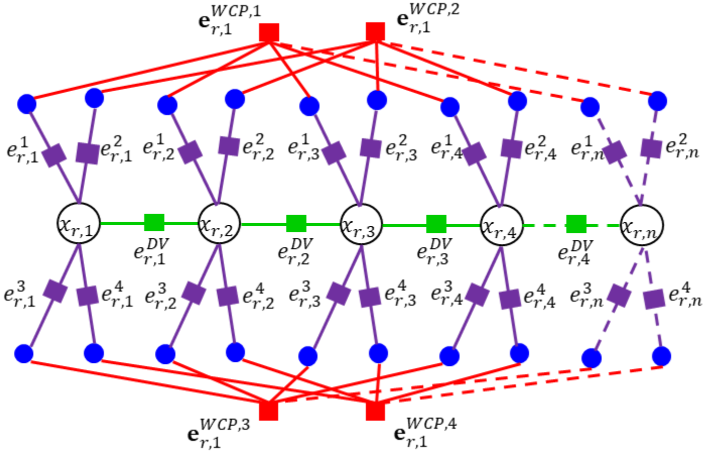

The continuous observed carrier-phase measurements between multiple epochs:

$$\begin{bmatrix} \lambda\psi^1_{r,1} \\ \lambda\psi^1_{r,2} \\ \ldots \\ \lambda\psi^1_{r,N^s_k} \end{bmatrix} = \begin{bmatrix} r^s_{r,t} + m^s_{r,1} \\ r^s_{r,2} + m^s_{r,2} \\ \ldots \\ r^s_{r,N^s_k} + m^s_{r,N^s_k} \end{bmatrix} + \begin{bmatrix} \lambda B^s_{r,1} \\ \lambda B^s_{r,2} \\ \ldots \\ \lambda B^s_{r,N^s_k} \end{bmatrix} + \begin{bmatrix} \epsilon^s_{r,1} \\ \epsilon^s_{r,2} \\ \ldots \\ \epsilon^s_{r,N^s_k} \end{bmatrix}$$

With $m^s_{r,t} = c_L(\delta_{r,t} - \delta^s_{r,t}) - I^s_{r,t} + T^s_{r,t} + d\psi^s_{r,t}$

WCP Factor for the given measurements $(\lambda\psi^1_{r,t}, \lambda\psi^1_{r,t+1}, \ldots \lambda\psi^1_{r,N}$

$$\left\|\mathbf{e}^{WCP,s}_{r,k}\right\|^2_{\boldsymbol{\Sigma}^{WCP,s}_{r,k}} = \left\| \mathbf{G}^s_{r,k} \begin{bmatrix} \lambda\psi^1_{r,1} \\ \lambda\psi^1_{r,2} \\ \ldots \\ \lambda\psi^1_{r,N^s_k} \end{bmatrix} - \mathbf{G}^s_{r,k} \begin{bmatrix} h^{WCP,s}_{r,1}(\mathbf{p}_{r,1}, \mathbf{p}^s_1, \delta_1) \\ h^{WCP,s}_{r,2}(\mathbf{p}_{r,2}, \mathbf{p}^s_2, \delta_2) \\ \ldots \\ h^{WCP,s}_{r,N^s_k}(\mathbf{p}_{r,N^s_k}, \mathbf{p}^s_{N^s_k}, \delta_{N^s_k}) \end{bmatrix} \right\|^2_{\boldsymbol{\Sigma}^{WCP,s}_{r,k}}$$

$$\boldsymbol{\Sigma}^{WCP,s}_{r,k} = \mathbf{G}^s_{r,k} \begin{bmatrix} \epsilon^s_{r,1} & 0 & 0 & 0 \\ 0 & \epsilon^s_{r,2} & 0 & 0 \\ 0 & 0 & \ldots & 0 \\ 0 & 0 & 0 & \epsilon^s_{r,N^s_k} \end{bmatrix} \mathbf{G}^{s\ \mathrm{T}}_{r,k}$$

$\mathbf{p}_{r,N^s_k}$: receiver r position
$\mathbf{p}^s_{N^s_k}$: satellite s position
$\delta_{N^s_k}$: the clock bias
B^s_{r,N^s_k} : the shared integer ambiguity
$d\psi^s_{r,t}$: the carrier phase correction
$\epsilon^s_{r,t}$: the errors caused by multipath

The N^s_k indicates that satellite 1 is tracked continuously for N^s_k epochs

$\boldsymbol{\Sigma}^{WCP,s}_{r,k}$ and $\boldsymbol{\Sigma}^{TDCP,s}_{r,k}$ denote **covariance matrix** calculated by the satellite elevation angle, signal, and noise ratio

Comparison between the proposed WCP and TDCP

WCP (aided by left null space matrix)

$$\mathbf{G}^{s}_{r,k}\begin{bmatrix}\lambda\psi^{1}_{r,1}\\ \lambda\psi^{1}_{r,2}\\ \dots\\ \lambda\psi^{1}_{r,N^{s}_{k}}\end{bmatrix}=\mathbf{G}^{s}_{r,k}\begin{bmatrix}r^{s}_{r,t}+m^{s}_{r,1}\\ r^{s}_{r,2}+m^{s}_{r,2}\\ \dots\\ r^{s}_{r,N^{s}_{k}}+m^{s}_{r,N^{s}_{k}}\end{bmatrix}+\mathbf{G}^{s}_{r,k}\begin{bmatrix}\epsilon^{s}_{r,1}\\ \epsilon^{s}_{r,2}\\ \dots\\ \epsilon^{s}_{r,N^{s}_{k}}\end{bmatrix}$$

TDCP

$$\Delta\lambda\psi^{s}_{r,t,t+1}=(r^{s}_{r,t+1}-r^{s}_{r,t})+c_{L}\left(\delta_{r,t+1}-\delta_{r,t}\right)+(\epsilon^{s}_{r,t+1}-\epsilon^{s}_{r,t})$$

Cross-correlation Matrix

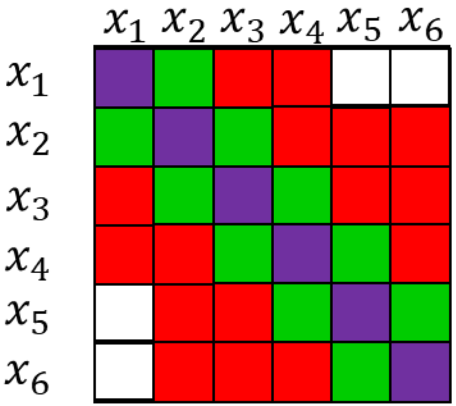

Dense matrix

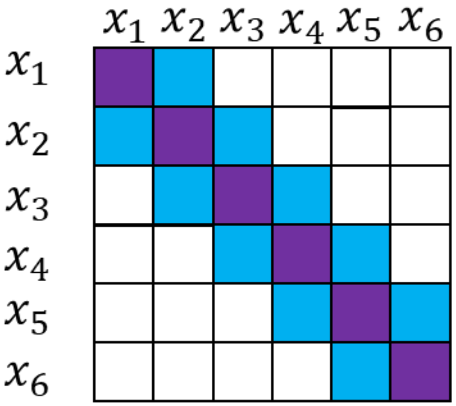

Sparse matrix

the TDCP can be a special format of the WCP constraint with a window size of 2

According to the nature of GNSS tracking loops, **the integer ambiguity tends to be constant** when the satellite is **effectively tracked !**

Potential cycle slip

Cycle Slip Accommodation

☒ shared integer ambiguity inside a WCP

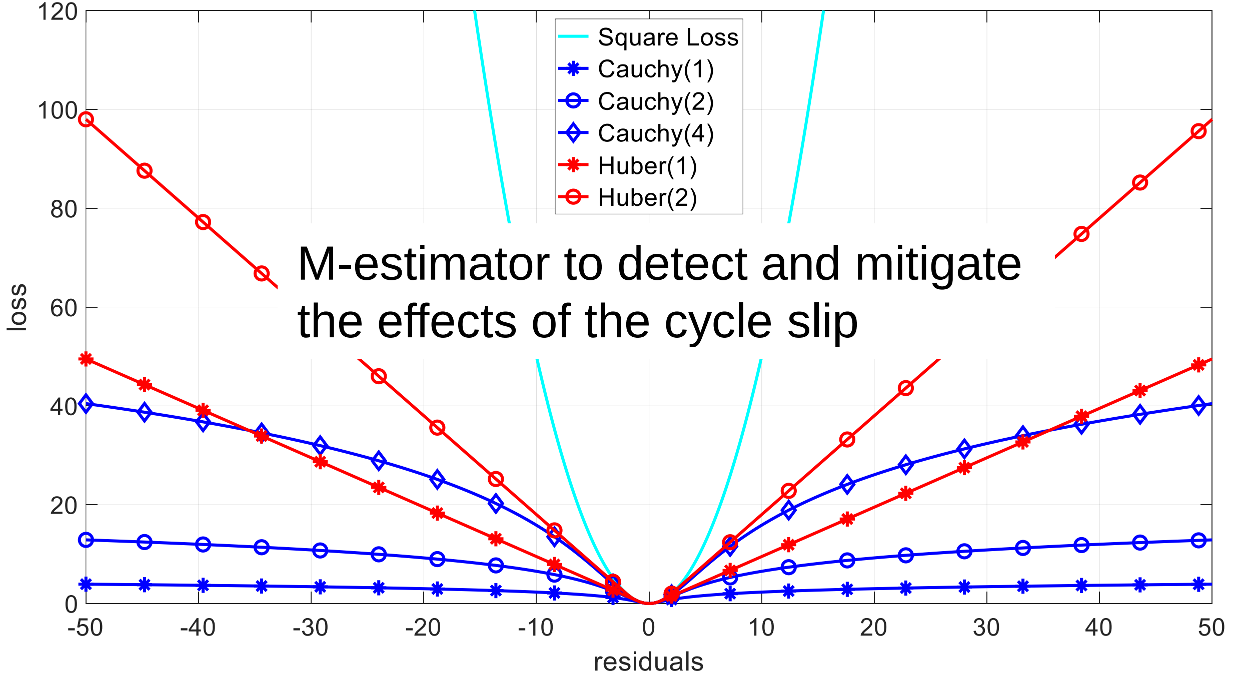

M-estimator to detect and mitigate the effects of the cycle slip

$$\rho(r) = \frac{{k_\rho}^2}{2}\log(1 + \frac{(r)^2}{{k_\rho}^2})$$

Comparisons of the robust functions with different kernel values (k_ρ).

Factor Graph Structure (Pseudorange/Doppler/WCP)

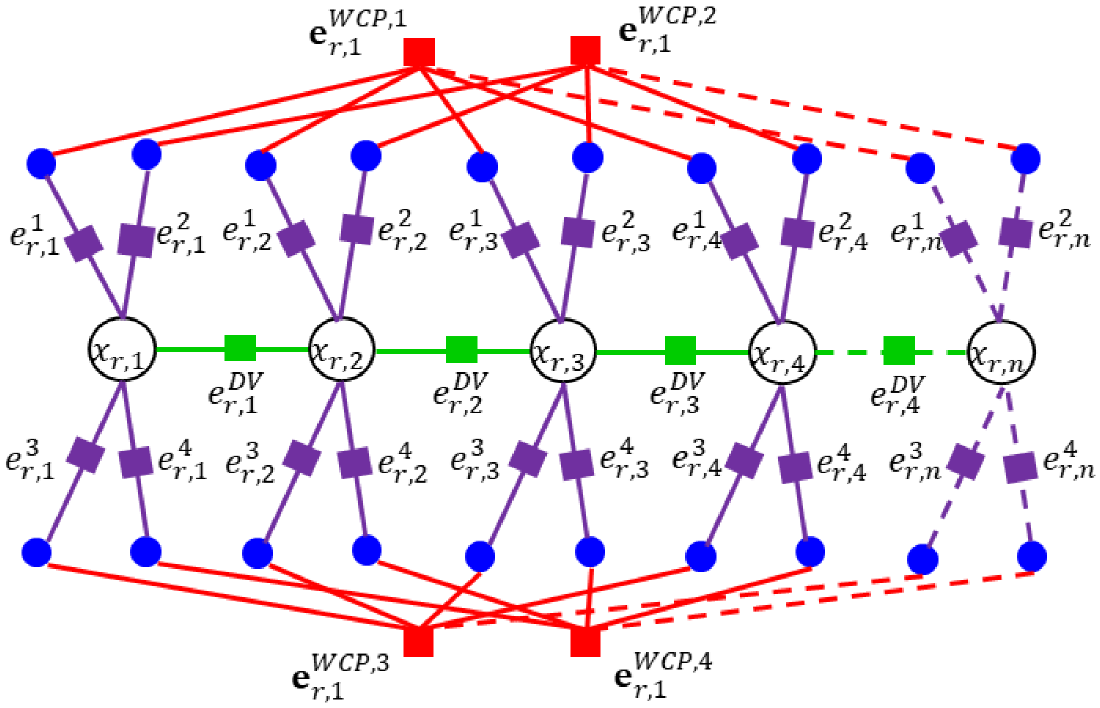

- Pseudorange Factor: $e^{s}_{r,t}$
- Doppler Velocity Factor: $e^{DV}_{r,t}$
- WCP Factor: $\mathbf{e}^{WCP,s}_{r,t}$

$$\chi^* = \arg\min_{\chi} \sum_{s,t,k} \left(\left| \mathbf{e}^{DV}_{r,t} \right|^2_{\Sigma^{DV}_{r,t}} + \left| \mathbf{e}^{s}_{r,t} \right|^2_{\Sigma^{s}_{r,t}} + \left| \rho\left(\mathbf{e}^{WCP,s}_{r,k}\right) \right|^2_{\Sigma^{WCP,s}_{r,k}} \right)$$

$$\rho\left(\mathbf{e}^{WCP,s}_{r,k}\right) = \frac{{k_\rho}^2}{2}\log\left(1 + \frac{(\mathbf{e}^{WCP,s}_{r,k})^2}{{k_\rho}^2}\right)$$

Experiment Setup

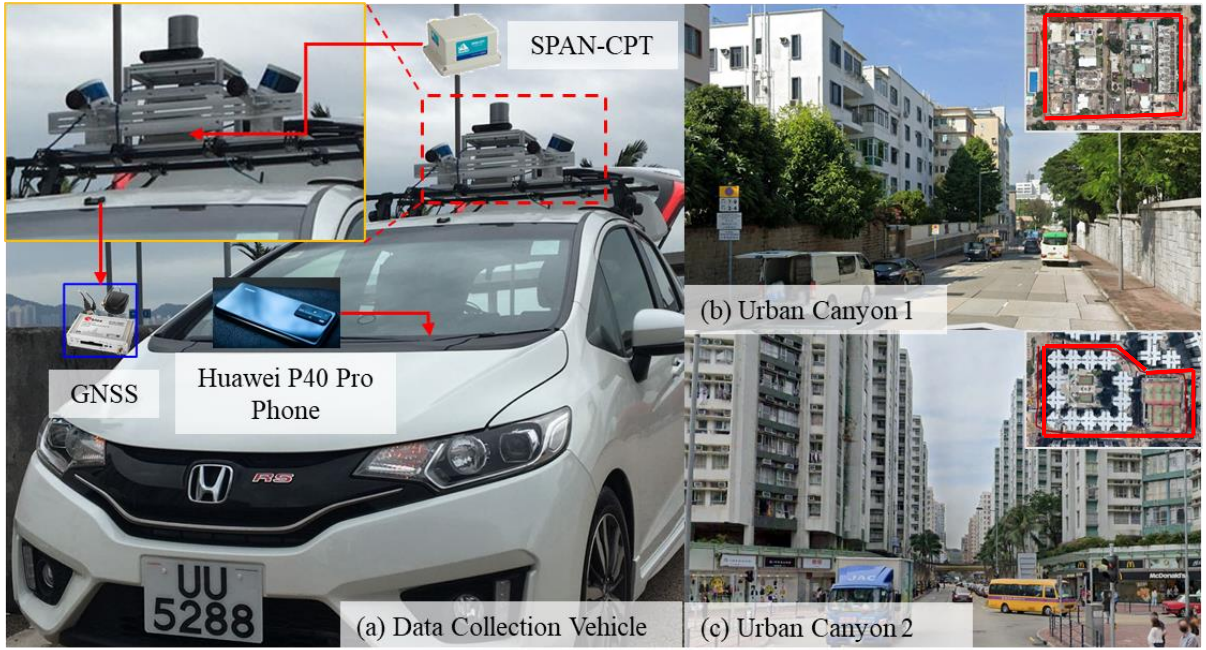

The evaluated **urban canyons 1 and 2**. The red curves inside the Figures denote the trajectories of the tests.

We analyze the performance of positioning by comparing five different methods:

(a) **u-blox**

(b) **WLS**

(c) **PSR-DOP (Sol 1)**

the pseudorange and Doppler integration using FGO

(d) **PSR-DOP-TDCP (Sol 2)**

the pseudorange, Doppler, and TDCP measurements integration

(e) **PSR-DOP-WCP (Sol 3)**

the pseudorange, Doppler, and WCP measurements integration

Experiment Results in Urban Canyon 1

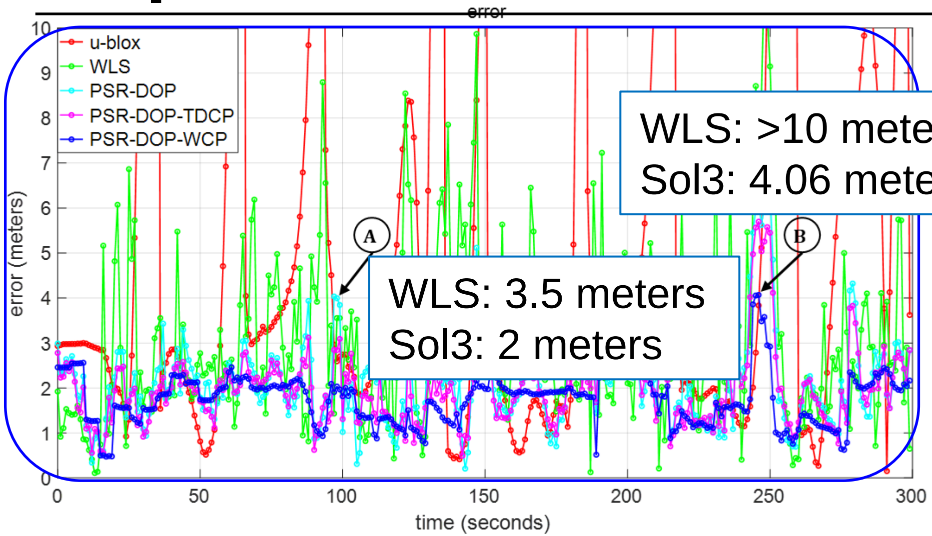

Performance of the listed five methods in urban canyon 1

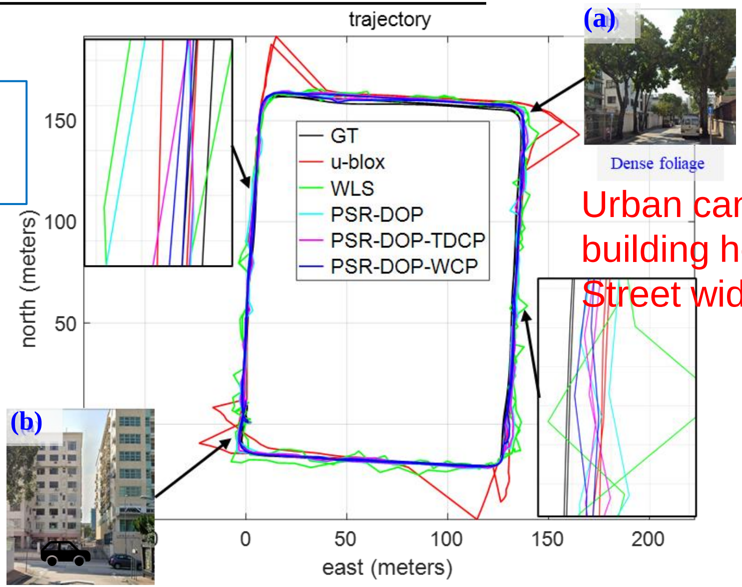

Urban canyon 1:
building height is 16 m
Street width is 15 m

Item (m)	u-blox	WLS	Sol 1	Sol 2	Sol 3
MEAN	6.23	3.10	2.14	2.01	1.76
STD	7.31	1.95	1.01	0.82	0.57
Max	38.53	11.23	6.52	5.69	4.06

The improvement of our proposed method (Sol3) can reach 71.7%, compared to the method of u-blox

Almost a lane-level accuracy

Analysis of Impact of Maximum Window Size

Positioning errors of the proposed method under different $N_{k,MAX}^{S}$

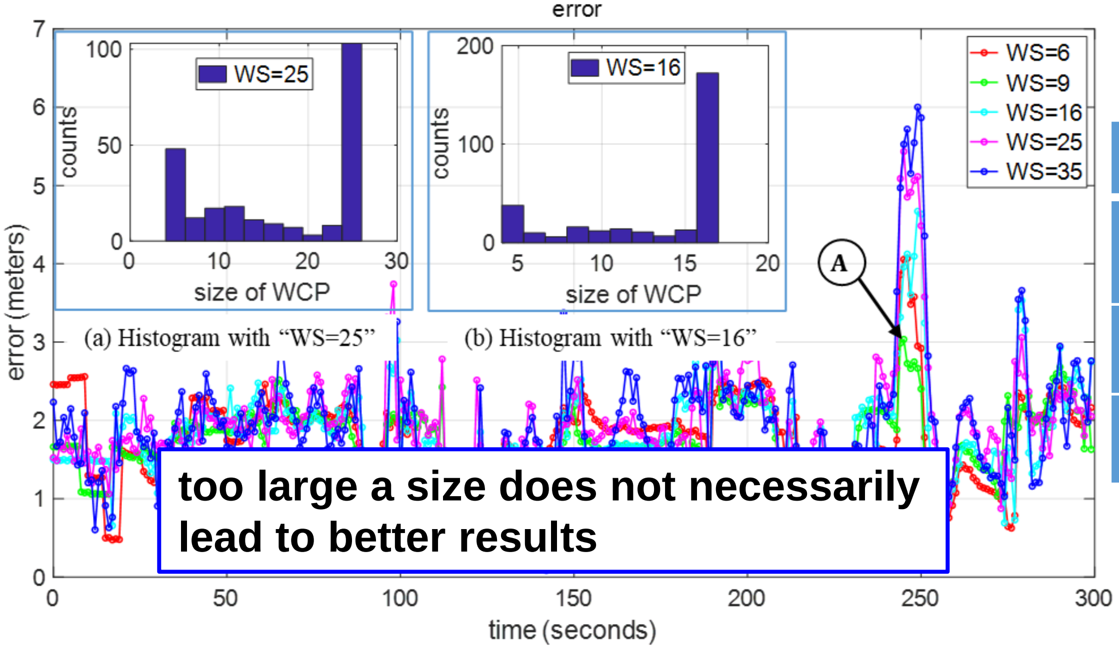

too large a size does not necessarily lead to better results

WS: maximum window size ($N_{k,MAX}^{S}$)

Due to the potential cycle slips violate the shared integer ambiguity

$N_{k,MAX}^{S}$	6	9	16	25	35
MEAN (m)	1.76	1.69	1.82	1.89	1.93
STD (m)	0.57	0.48	0.62	0.72	0.82
Max (m)	4.06	3.16	4.67	5.43	6.01

The larger $N_{k,MAX}^{S}$ enables the stronger correlation between the states

Cycle Slip Accommodation

☒ shared integer ambiguity inside a WCP

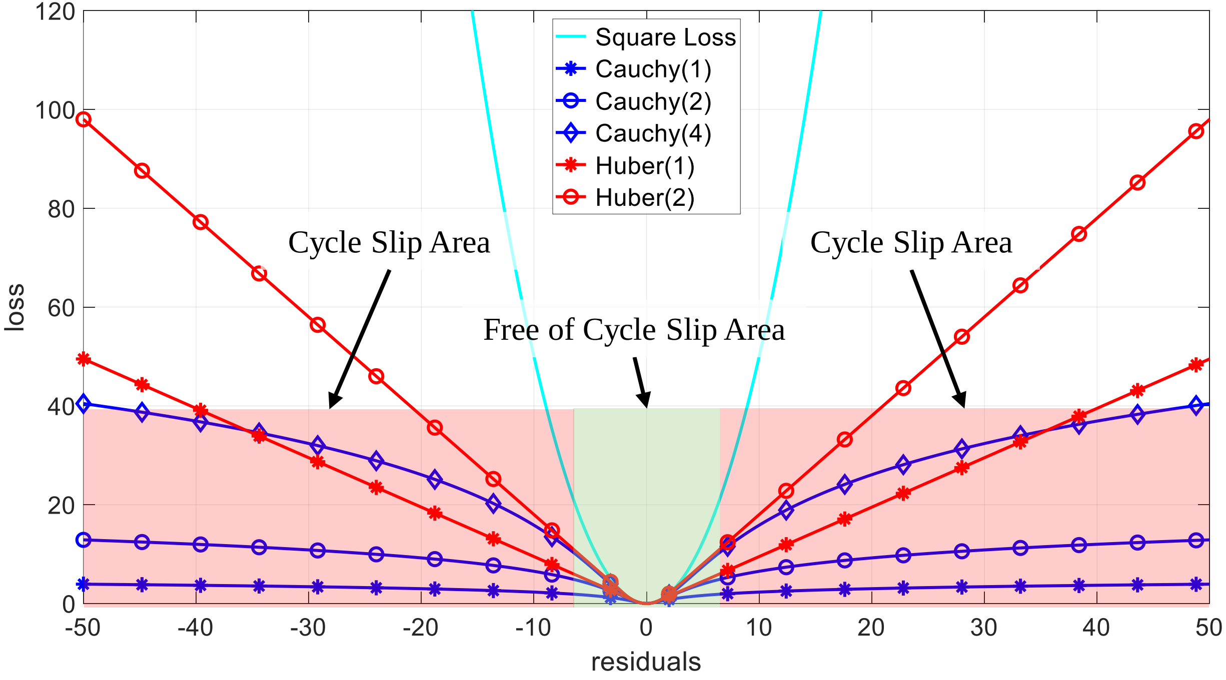

Comparisons of the robust functions with different kernel values (k_ρ)

M-estimator to detect and mitigate the effects of the cycle slip

$$\rho\left(\mathbf{e}_{r,k}^{WCP,s}\right) = \frac{{k_\rho}^2}{2}\log\left(1 + \frac{(\mathbf{e}_{r,k}^{WCP,s})^2}{{k_\rho}^2}\right)$$

$$\left\|\mathbf{e}_{r,k}^{WCP,s}\right\|^2_{\Sigma_{r,k}^{WCP,s}} = \left\| \mathbf{G}_{r,k}^{s}\begin{bmatrix}\lambda\psi_{r,1}^{1}\\ \lambda\psi_{r,2}^{1}\\ \cdots\\ \lambda\psi_{r,N_k^s}^{1}\end{bmatrix} - \mathbf{G}_{r,k}^{s}\begin{bmatrix}h_{r,1}^{WCP,s}(\mathbf{p}_{r,1}, \mathbf{p}_1^s, \delta_1)\\ h_{r,2}^{WCP,s}(\mathbf{p}_{r,2}, \mathbf{p}_2^s, \delta_2)\\ \cdots\\ h_{r,N_k^s}^{WCP,s}(\mathbf{p}_{r,N_k^s}, \mathbf{p}_{N_k^s}^s, \delta_{N_k^s})\end{bmatrix}\right\|^2_{\Sigma_{r,k}^{WCP,s}}$$

Cycle Slip Accommodation

Analysis of the Cycle Slip Accommodation via M-estimator

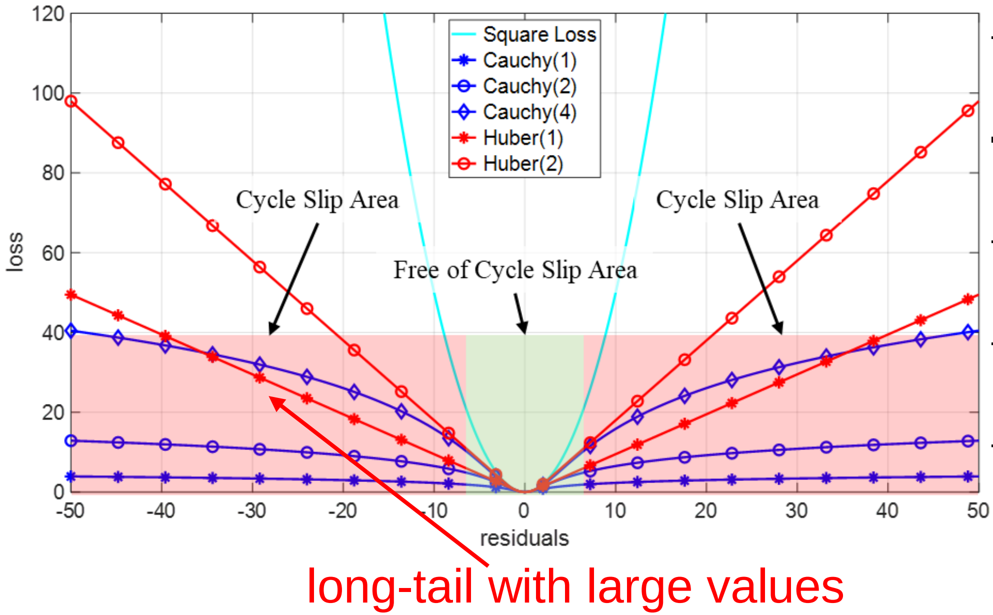

Item (m)	H (1)	H (2)	C (1)	C (2)	C (4)
MEAN	Diverge	Diverge	3.62	3.11	3.05
STD	Diverge	Diverge	2.04	1.78	1.68
Max	Diverge	Diverge	13.11	11.20	10.76

Positioning error of the Sol3 under different M-estimator setups in urban canyon 2

Which one best ?

Cycle Slip Mitigation in Urban Canyon 2

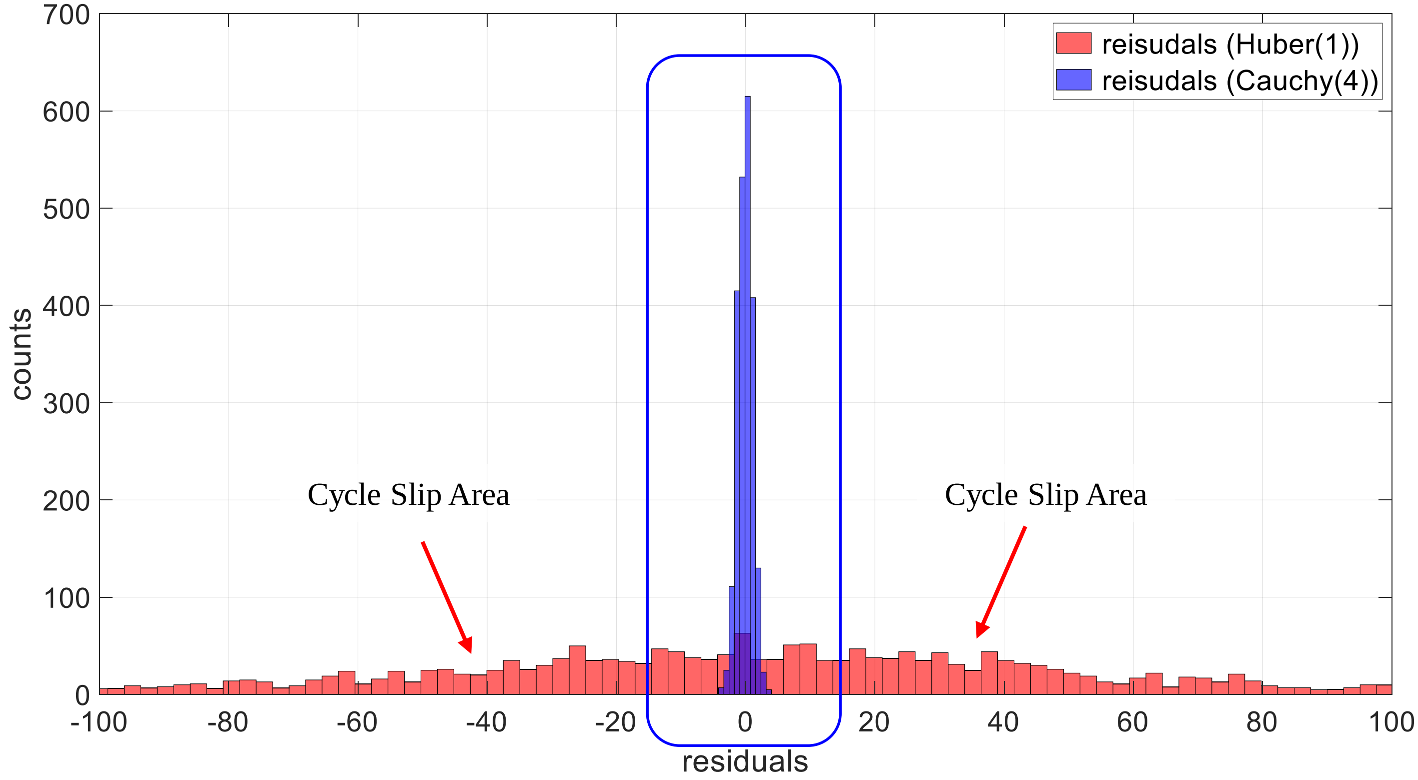

Histograms of residuals of the WCP constraints using the Cauchy and Huber functions

Experiment Results in Urban Canyon 2

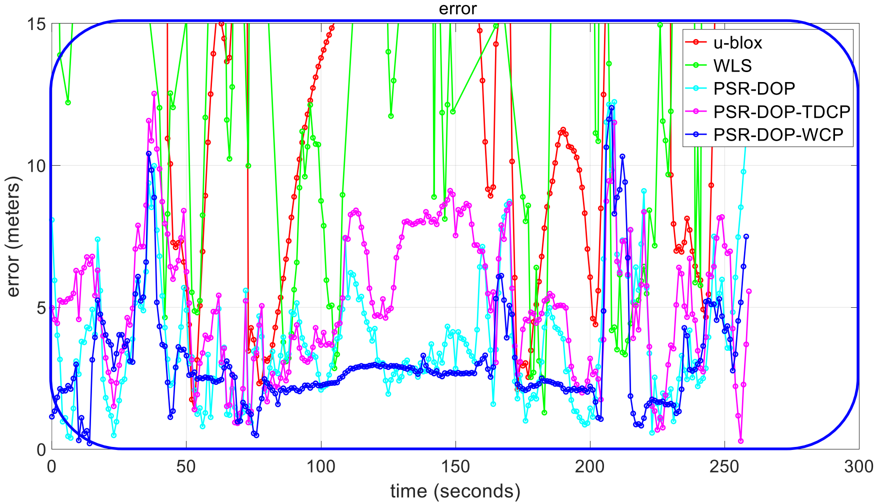

Performance of the listed five methods in urban canyon 2

Item (m)	u-blox	WLS	Sol 1	Sol 2	Sol 3
MEAN	31.02	16.66	3.90	5.21	2.96
STD	37.69	12.82	2.29	2.38	1.89
Max	177.6	56.23	12.84	12.52	12.02

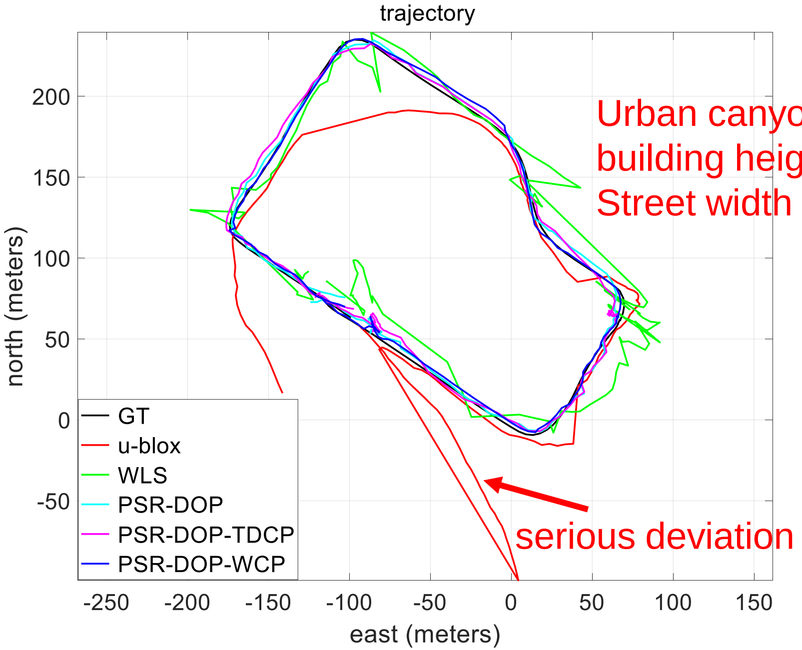

Urban canyon 2:
building height is 35 m
Street width is 22 m

The improvement of our proposed method (Sol3) ca
reach 90.5%, compared to the method of u-blox

Experiment results by Huawei P40 phone

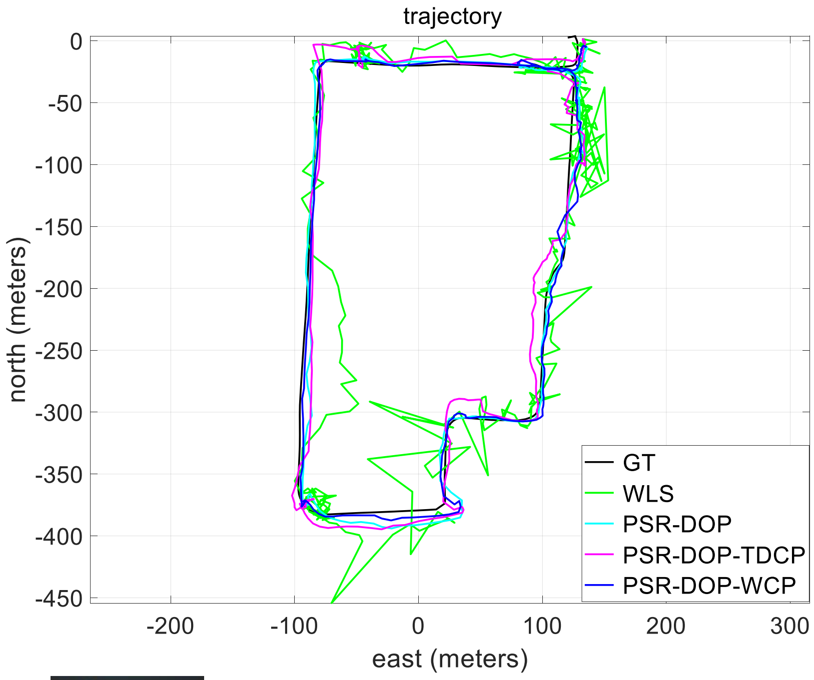

Performance of the listed four methods in the urban canyon

Item (m)	WLS	Sol 1	Sol 2	Sol 3
MEAN	14.45	8.74	9.19	7.47
STD	11.79	4.21	4.82	4.60
Max	110.74	46.10	45.39	46.38

The improvement of our proposed method (Sol3) can reach 48.3%, compared to the method of WLS

Low-cost Smartphone-level Receiver

Huawei P40 Pro Phone

Brief Summary

- Solved Problems: Exploitation of time-correlation of carrier measurements
- Limitations: Relying on the assumption of constant integer ambiguity for the continuously observed carrier-phase measurements.
- Future work: How to detect the cycle slip of the carrier phase measurements in urban canyons

APPENDIX-Discussion

Performance Comparison of the Loosely and Tightly Integrated Doppler Measurements in FGO

Item	PSR-DOP	PSR-DOP-TC
MEAN (meter)	2.14	2.01
STD (meter)	1.01	0.91
Max (meter)	6.52	5.6
Used Time Per Epoch (ms)	51	125

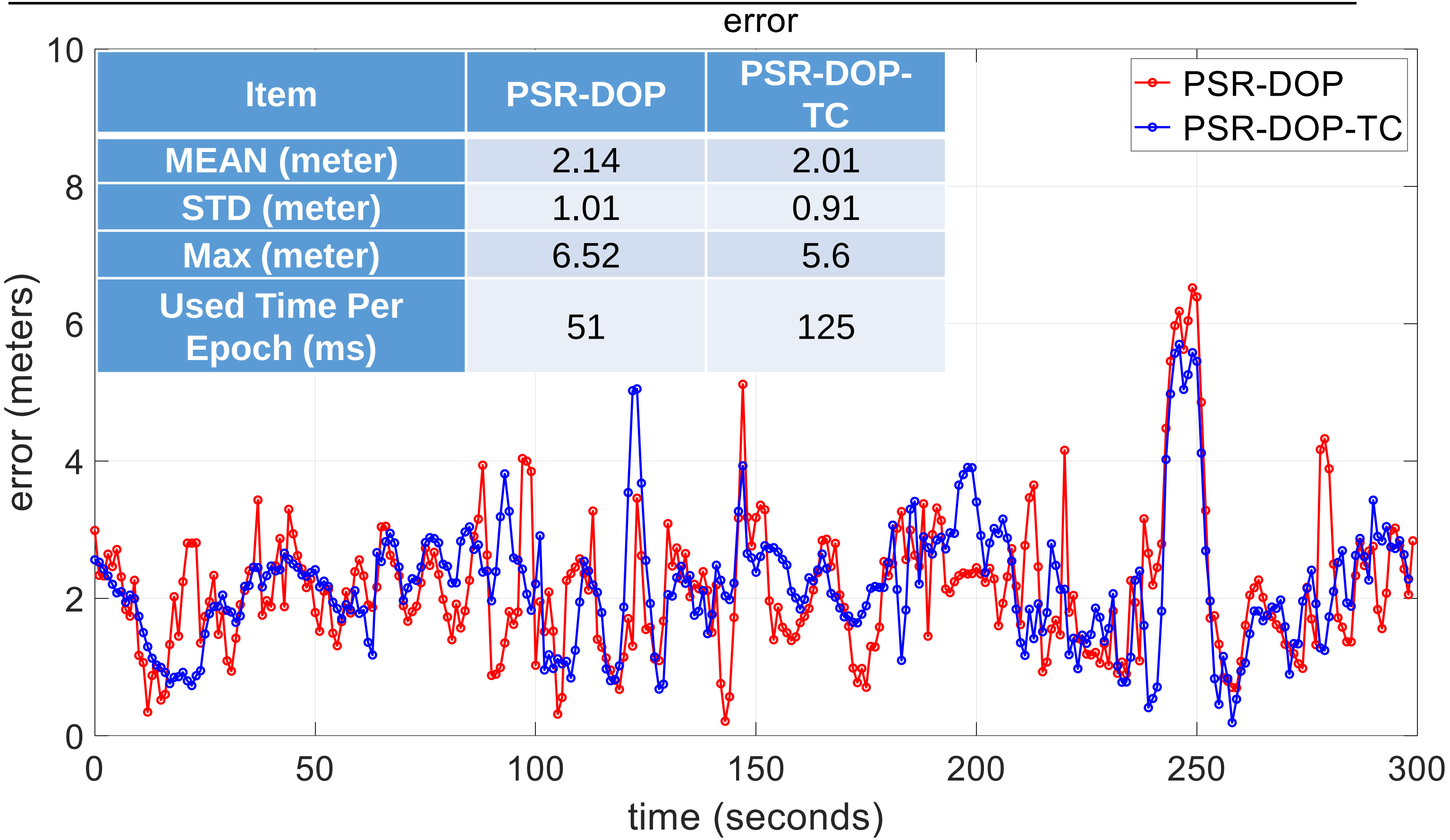

APPENDIX-Discussion

Performance Comparison of the Cycle Slip Mitigation Using M-estimator and loop lock indicator (LLI)

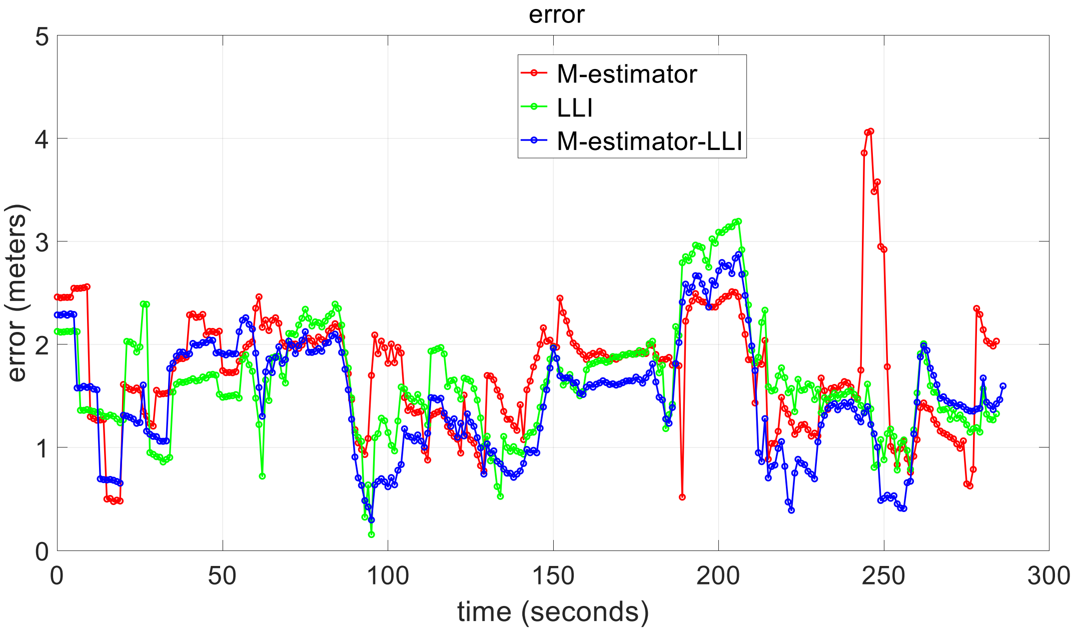

LLI :one of the popular methods for cycle slip detection, can be directly output from receiver

The implementation is based on PSR-DOP-WCP

Item (m)	M-estimator	LLI	M-estimator-LLI
MEAN	1.76	1.64	1.47
STD	0.57	0.53	0.56
Max	4.06	3.19	2.87

Cycle slip detection

a new WCP constraint will be generated

Thank you !

Q & A